ARTICLE
Journal of Cellular Biochemistry 113:3380–3392 (2012)

Journal of Cellular Biochemistry

Modeling Human Osteosarcoma in Mice Through 3AB-OS Cancer Stem Cell Xenografts

Riccardo Di Fiore,[1] Annalisa Guercio,[2] Roberto Puleio,[2] Patrizia Di Marco,[2] Rosa Drago-Ferrante,[1] Antonella D'Anneo,[1] Anna De Blasio,[1] Daniela Carlisi,[1] Santina Di Bella,[1] Francesca Pentimalli,[3] Iris M. Forte,[3] Antonio Giordano,[3,4,5] Giovanni Tesoriere,[1] and Renza Vento[1,4*]

[1] *Section of Biochemical Sciences, Department of Experimental Biomedicine and Clinical Neurosciences, University of Palermo, Via del Vespro 129, Polyclinic, 90127 Palermo, Italy*

[2] *Istituto Zooprofilattico Sperimentale della Sicilia "A.Mirri", Via Gino Marinuzzi 3, 90129 Palermo, Italy*

[3] *INT-CROM, 'Pascale Foundation', National Cancer Institute - Cancer Research Center, Via Ammiraglio Bianco-83013, Mercogliano, Avellino, Italy*

[4] *Sbarro Institute for Cancer Research and Molecular Medicine, College of Science and Technology, Temple University, Philadelphia, Pennsylvania 19122*

[5] *Department of Human Pathology and Oncology, University of Siena, Policlinico "Le Scotte", Siena, Italy*

ABSTRACT

Osteosarcoma is the second leading cause of cancer-related death for children and young adults. In this study, we have subcutaneously injected—with and without matrigel—athymic mice (Fox1nu/nu) with human osteosarcoma 3AB-OS pluripotent cancer stem cells (CSCs), which we previously isolated from human osteosarcoma MG63 cells. Engrafted 3AB-OS cells were highly tumorigenic and matrigel greatly accelerated both tumor engraftment and growth rate. 3AB-OS CSC xenografts lacked crucial regulators of beta-catenin levels (E-cadherin, APC, and GSK-3beta), and crucial factors to restrain proliferation, resulting therefore in a strong proliferation potential. During the first weeks of engraftment 3AB-OS-derived tumors expressed high levels of pAKT, beta1-integrin and pFAK, nuclear beta-catenin, c-Myc, cyclin D2, along with high levels of hyperphosphorylated-inactive pRb and anti-apoptotic proteins such as Bcl-2 and XIAP, and matrigel increased the expression of proliferative markers. Thereafter 3AB-OS tumor xenografts obtained with matrigel co-injection showed decreased proliferative potential and AKT levels, and undetectable hyperphosphorylated pRb, whereas beta1-integrin and pFAK levels still increased. Engrafted tumor cells also showed multilineage commitment with matrigel particularly favoring the mesenchymal lineage. Concomitantly, many blood vessels and muscle fibers appeared in the tumor mass. Our findings suggest that matrigel might regulate 3AB-OS cell behavior providing adequate cues for transducing proliferation and differentiation signals triggered by pAKT, beta1-integrin, and pFAK and addressed by pRb protein. Our results provide for the first time a mouse model that recapitulates in vivo crucial features of human osteosarcoma CSCs that could be used to test and predict the efficacy in vivo of novel therapeutic treatments. J. Cell. Biochem. 113: 3380–3392, 2012.

KEY WORDS: 3AB-OS CSCS; OSTEOSARCOMA; XENOGRAFT; MATRIGEL; ANIMAL MODELS

Conflicts of interest: None.

Additional supporting information may be found in the online version of this article.

Grant sponsor: Italian Ministry of Education, University and Research (MIUR) ex-60%, 2007; Grant sponsor: Innovative Research Projects (University of Palermo, Italy, 2007); Grant sponsor: MIUR-PRIN; Grant number: 2008P8BLNF (2008); Grant sponsor: MIUR; Grant number: 867/ 06/ 07/2011; Grant sponsor: MIUR; Grant number: 2223/12/19/2011; Grant sponsor: MIUR-PRIN; Grant number: 144/01/26/2012; Grant sponsor: Istituto Zooprofilattico Sperimentale della Sicilia "A.Mirri", Palermo, Italy.

*Correspondence to: Prof. Renza Vento, Section of Biochemical Sciences, Department of Experimental Biomedicine and Clinical Neurosciences, University of Palermo, Via del Vespro 129, 90127 Palermo, Italy.
E-mail: renza.vento@unipa.it

Manuscript Received: 28 May 2012; Manuscript Accepted: 31 May 2012

Accepted manuscript online in Wiley Online Library (wileyonlinelibrary.com): 11 June 2012

DOI 10.1002/jcb.24214 • © 2012 Wiley Periodicals, Inc.

Osteosarcoma, the most common of primary bone malignancies, is among a group of mesenchymal cancers characterized by clinical, histologic and molecular heterogeneity, and karyotypes with a high degree of aneuploidy [Smida et al., 2010]. It is a highly aggressive tumor with a high metastasizing potential and, at present, it remains the second leading cause of cancer-related death for children and young adults [Ta et al., 2009]. The current standard protocol of a three-drug chemotherapy regimen, using cisplatin, doxorubicin, and high-dose methotrexate, results in no more than 70% long-term disease-free survival for osteosarcoma patients without metastasis [Wesolowski and Budd, 2010]. There is no established second-line chemotherapy for relapsed osteosarcoma, and therefore new therapeutic approaches are urgently needed.

It is well established that most solid tumors are hierarchically organized and that their growth is sustained by a distinct subpopulation of cells, termed cancer stem cells (CSCs) [Clevers, 2011], which represent the source for tissue renewal and hold malignant potential [Li and Neaves, 2006; Maitland and Collins, 2008]. CSCs confer resistance to therapies; thus, a successful cure of cancer should require CSCs eradication.

We have recently demonstrated that prolonged treatments (about 100 days) of human osteosarcoma MG63 cells with 3-aminobenzamide (3-AB), a potent competitive inhibitor of poly(ADP-ribose)-polymerase (PARP), induce massive cell death followed by progressive enrichment of a new CSC population named 3AB-OS. This 3AB-OS CSC line [Di Fiore et al., 2009] has been recently patented (''Pluripotent cancer stem cells: Their preparation and use''. FI2008A000238. 11/12/2008. N. PCT/IB2009/055690, 11/12/2009) and represents a pluripotent, heterogeneous, and stable cell population, which has been characterized at the molecular [Di Fiore et al., 2009] and genetic level [Di Fiore et al., paper submitted]. Overall, our results have suggested that the original human osteosarcoma MG63 cells might contain a rare population of multipotent CSCs, which has been selected and enriched by 3AB treatment.

The translation of therapeutic strategies for osteosarcoma from the experimental phase into the clinic has been limited by insufficient animal models bearing the basic features of human tumors. Generating an appropriate and reliable experimental model of human cancer is crucial to identify and test possible antitumor strategies.

Xenograft models obtained through transplantation of cancer cell lines into immunodeficient mice are very useful to analyze the molecular mechanisms underlying tumor development and to identify novel molecular therapeutic approaches. Tumor cell xenografts can be readily accepted by immunocompromised mice, such as athymic nude mice bearing a genetic mutation that causes thymic aplasia and results in an inhibited immune system [Sharkey and Fogh, 1984]. The athymic nude mouse can receive many different types of tissue and tumor grafts providing a model that is easy to manage, easy to establish, and very effective for testing tumor treatments; it is characterized by a consistent and reproducible cell growth and permits easy access to the tumor for treatment, caliper measurement, and imaging evaluation, representing, therefore, a useful model for studying the biology and response to therapies of human tumors in vivo. Here, we report a xenograft model of human osteosarcoma CSCs that could be clinically relevant. Because of the distinctive capability of CSCs to recapitulate the development of the original tumors in vivo, human osteosarcoma 3AB-OS CSC xenografts into nude mice might provide an avenue for testing in vivo approaches to pathway-targeted drug discovery and preclinical screening and to investigate the behavior of human osteosarcoma CSCs.

MATERIALS AND METHODS

CELL LINES AND CULTURE CONDITIONS

The human osteosarcoma MG63 cells were acquired from Interlab Cell Line Collection (Genova, Italy). The human 3AB-OS CSCs were generated in our laboratory [Di Fiore et al., 2009]. 3AB-OS and MG63 cells were cultured as monolayers in Dulbecco's modified Eagle medium (DMEM), supplemented with 10% (v/v) heat inactivated fetal bovine serum, 2 mM L-glutamine, and penicillin–streptomycin antibiotics (50 μg/ml) (Euroclone, Pero, Italy) in a humidified atmosphere of 5% CO_2 in air at 37°C. When cells grew to approximately 80% confluence, they were subcultured or harvested using 0.25% trypsin-EDTA (Life Technologies Ltd).

MATRIGEL

BD Matrigel™, purchased from BD Biosciences- Discovery Labware, Becton Dickinson, (Buccinasco, Italy), is a solubilized basement membrane preparation extracted from the Engelbreth-Holm-Swarm (EHS) mouse sarcoma. It polymerizes under normal physiological conditions to produce a reconstituted, biologically active matrix, which favors cell attachment and differentiation. As BD Matrigel rapidly gels at 22–35°C, it was thawed overnight at 4°C, aliquoted on ice into pre-cooled sterile microcentrifuge tubes and then frozen at −20°C until use. All procedures involving Matrigel were carried out at 4°C on ice to prevent polymerization.

CELL LINES AND MOUSE XENOGRAFT GENERATION

MG63 and 3AB-OS cells were proven to be free of mycoplasma infection by reverse-transcriptase polymerase chain reaction (RTPCR) (Takara Shuzo Co, Ltd, Kyoto, Japan) of supernatant from densely growing cells. MG63 and 3AB-OS cells to be implanted were harvested at approximately 80% confluence, washed in phosphate-buffered saline (PBS) (Life Technologies Ltd), resuspended in serum-free culture medium, counted in a hemocytometer, and equilibrated at a density of 3×10^6 cells per 150 μl DMEM. Cell viability was assessed through trypan blue staining.

MG63 cells and 3AB-OS cells (3×10^6) were both prepared in either DMEM or DMEM/Matrigel (1/1 mixture), into a final volume of 300 μl for injection. Cells were injected subcutaneously into the flank of 4-week old male athymic nude mice. Male athymic nude mice (*Foxn1*nu/nu), carrying a disruption of the forkhead box n1 gene [Coffer and Burgering, 2004], which leads to thymic atrophy and immunodeficiency [Nehls et al., 1996], were purchased from Harlan, Udine, Italy. Mice were acclimated for 1 week before the start of this study. All animals have received humane care in compliance with the ''Guide for the Care and Use of Laboratory Animals'' published by the National Institutes of Health. The authors have received prior permission from their Institutional Animal Care & Use

Committee (IACUC). Dr. Patrizia Di Marco was the accredited veterinarian.

Fifteen animals were used for each treatment group as reported in results. Animals were kept in a light- and temperature-controlled environment and provided with food and water ad libitum.

MOUSE HEALTH AND CONDITION ASSESSMENT AND TUMOR MEASUREMENT

Mice were inspected for tumor appearance, by daily observation and palpation. To minimize pain, discomfort, and distress, all mice were observed daily for their behavior and body weight (BW)—recorded every week—was used as an index of mice-welfare. BCS, which ranges from 1 (emaciation) to 5 (obesity), was determined by visual and hands-on examination of each animal. The hands-on examination was done by holding the mouse by the base of the tail and passing a finger over the sacroiliac bones and vertebral column [Ullman-Culleré and Foltz, 1999]. We established that BCS had not to exceed 2, with BCS = 2 corresponding to "underconditioned" (with segmentation of vertebrae and dorsal pelvic bones readily palpable), and the mean tumor size had not to exceed 10% of the mouse BW. Tumor volume was calculated through an external caliper, measuring twice weekly the greatest longitudinal diameter (length) and the greatest transverse diameter (width) and volumes were calculated by the formula "Tumor volume (mm^3) = $width^2 \times length \times 0.52$ [Euhus et al., 1986; Tomayko and Reynolds, 1989]. Mice were sacrificed by cervical dislocation and tumor samples and tissues were collected at 3, 5, and 7 weeks after cell injection.

TUMOR AND TISSUE HISTOLOGY, HISTOCHEMICAL, AND IMMUNOHISTOCHEMICAL STAINING

Tumors and tissues (hearts, lungs, kidneys, spleens, livers, and brains) were processed for macroscopic and histological examination. For light microscopy examination, tumors and tissues were fixed with 10% phosphate-buffered formalin and embedded in paraffin. Sections (4 μm thick) were cut and stored at room temperature until use. Routine histology (hematoxylin–eosin staining, H&E) was performed in order to evaluate basic histomorphological features of the specimens. The avidin-biotin-peroxidase complex (LSAB, Dako Corp., Santa Barbara, CA) method was used for immunohistochemical analyses. Tissue sections were sequentially dewaxed through a series of xylene, graded alcohol, and water immersion steps. Antigen was retrieved in citrate buffer (pH 6.0) microwave digestion (2 cycles of 5 min each, 750 W). Endogenous peroxide activity was suppressed by incubating the sections with 0.3% hydrogen peroxidase in methanol for 30 min at room temperature. After three × 10-min rinses in PBS, all tissue sections were incubated with 1% bovine serum albumin for 30 min at room temperature. Primary antibodies used in this study and their specific dilutions are summarized in Supplementary Table 1. Primary antibodies were diluted in PBS with 10.1% normal albumin serum and were incubated overnight at 4°C. After incubation, the slides were rinsed three times with PBS for 5 min, and incubated for 30 min at room temperature with the specific biotinylated secondary anti-rabbit, anti-goat, or anti-mouse antibody (LSAB, Dako Corp., Santa Barbara, CA). After two × 5-min rinses with PBS, tissue sections were incubated in PBS for 1 h at room temperature with streptavidin, horseradish peroxidase conjugate. All tissue sections were rinsed three times with Tris-buffer saline (TBS), incubated with the chromogen 3-3′-diaminobenzidine tetrahydrochloride (DAB; Dako) diluted 0.035% in TBS for 1 min, rinsed in tap water, and counterstained with Mayer's hematoxylin. The specific primary antibodies were replaced by PBS or normal goat serum in tissue sections used as negative controls.

Criteria to indicate marker expression in this study were as follows: The number of positive cells was semiquantitatively evaluated by counting the number of stained cells in 8–10 randomly chosen fields, counting at least 1,000 cells, at high magnification (40× objective and 10× eyepiece); four degrees of positivity for PCNA and Ki-67 were identified: "−" (0–24%), "+" (25–50%), "++" (51–74%), "+++" (75–100%); four degrees for other markers were identified: "−" no positive cell, "+" ≤30%, "++" 31–70%, and "+++" ≥71%.

Images of stained tissues were captured using Leica DMR microscope equipped with a Leica DFC 320 digital camera. The images were visualized with epifluorescent filters and transferred to Adobe Photoshop CS4 (Adobe Systems, San Jose, CA).

MITOSIS COUNT

Mitoses were counted in five fields (×40 lens) on replicate sections stained with toluidine blue which enhances the detection of mitotic figures.

RNA EXTRACTION AND REAL-TIME QUANTITATIVE RT-PCR

RNA was extracted from four 20 μm formalin-fixed paraffin-embedded (FFPE) sections for each sample. Paraffin was removed by xylene extraction followed by ethanol wash. RNA was isolated from sectioned tissue blocks using the RecoverAll™ Total Nucleic Acid Isolation Kit (Ambion, Life Technologies Corporation); a DNase I treatment step was included. One microgram of total RNA was reverse transcribed in a final volume of 20 μl Reverse transcription (RT) by using a Super-Script First-Strand Synthesis kit for RT-PCR (Invitrogen), according to the manufacturer's instructions. The resulting cDNAs were used for Quantitative real-time PCR (qPCR) using the primers (Proligo, Milan, Italy) reported in Supplementary Table 2 and the Power SYBR® Green PCR Master Mix (Applied Biosystem, Warrington, UK). Reactions were performed in 48-well plates according to manufacturer's instructions, using Applied Biosystems StepOne™ instrument. Each reaction mixture contained 2 μl of template cDNA, 12.5 μl of SYBR Green PCR Master Mix 2×, a final concentration of 300 nM of forward and reverse primers and RNase-free dH2O to a final volume of 25 μl. qPCRs were performed in triplicate and repeated for confirmation. PCR cycling was performed as follows: 95°C for 10 min; 95°C for 30 s, 60°C for 60 s, and 72°C for 30 s for 40 cycles; and a final extension at 72°C for 5 min. To determine primer specificity, three stages (95°C for 15 s, 60°C for 20 s, and 95°C for 15 s, with a ramping time of 20 min) were added at the end of the PCR to obtain dissociation curves for each gene. To verify that the RT-PCR signals derived from RNA rather than genomic DNA, for each gene tested a control identical to the test assay but omitting the RT reaction (no RT control) was included. qPCR data were analyzed by SDS 2.1 software. Relative transcript

TABLE I. Evaluation of In Vivo Tumorigenicity of MG63 and 3AB-OS Cells

Inoculation	Tumors/ mice	Tumor volume (mm^3)/3 weeks	Tumor weight (gr)/3 weeks	Tumor volume (mm^3)/5 weeks	Tumor weight (gr)/5 weeks	Tumor volume (mm^3)/7 weeks	Tumor weight (gr)/7 weeks
–	0/15	–	–	–	–	–	–
Matrigel	0/15	–	–	–	–	–	–
MG63 cells	0/15	–	–	–	–	–	–
MG63 cells + matrigel	0/15	–	–	–	–	–	–
3AB-OS cells	11/15	117	0.1	1,400	1.197	3,420	2.923
3AB-OS cells + matrigel	15/15	1,520*	1.29	3,610*	3.080	–	–

*$P < 0.05$.

levels were determined using the $2^{-\Delta\Delta Ct}$ method and normalized to endogenous β-actin control.

STATISTICAL ANALYSIS

Data were expressed as mean ± SE. Results of in vivo tumorigenicity assays and real-time RT-PCR analyses were evaluated by Student's *t*-test. Differences were considered significant when $P < 0.05$.

RESULTS

EVALUATION OF IN VIVO TUMORIGENICITY OF MG63 CELLS AND 3AB-OS CSCS

We have previously shown [Di Fiore et al., 2009] that 3AB-OS osteosarcoma cells possess in vitro the most significant properties of CSCs, including the ability to initiate tumors. Here, we have examined in vivo, in xenografted nude mice, the tumor-initiating capacity of both human osteosarcoma 3AB-OS CSCs and parental human osteosarcoma MG63 cells. To examine the tumorigenic potential of both cell lines (MG63 and 3AB-OS) 3×10^6 cells were mixed with either matrigel or cell culture medium and injected subcutaneously into 4 week-old immunocompromised mice. As reported in Table I, mice were subdivided into six groups, each composed of 15 mice. Each group was then further divided into three subgroups corresponding to the times when mice were sacrificed, i.e., at the end of the 3rd, 5th, and 7th week following inoculation (mice were 7, 9, and 11 week-old, respectively), if allowed by health conditions and ethical reasons. Control animals were either un-inoculated or inoculated with matrigel. Figure 1A is a representative picture of animals of each group subcutaneously inoculated with cancer cells. As shown in both Table I and Figure 1A, none of the mice inoculated with matrigel alone (0/15) or with MG63 cells alone (0/15) developed tumors. Even if some mice (4/15) co-inoculated with MG63 cells and matrigel developed a modest subcutaneous reaction (Fig. 1A), by histology it appeared to be composed of soft fatty tissue only (not shown). Instead, when mice were inoculated with 3AB-OS cells alone, tumors developed in 75% of mice (11/15 mice), or in 100% of mice (15/15 mice) when cells were injected in the presence of matrigel.

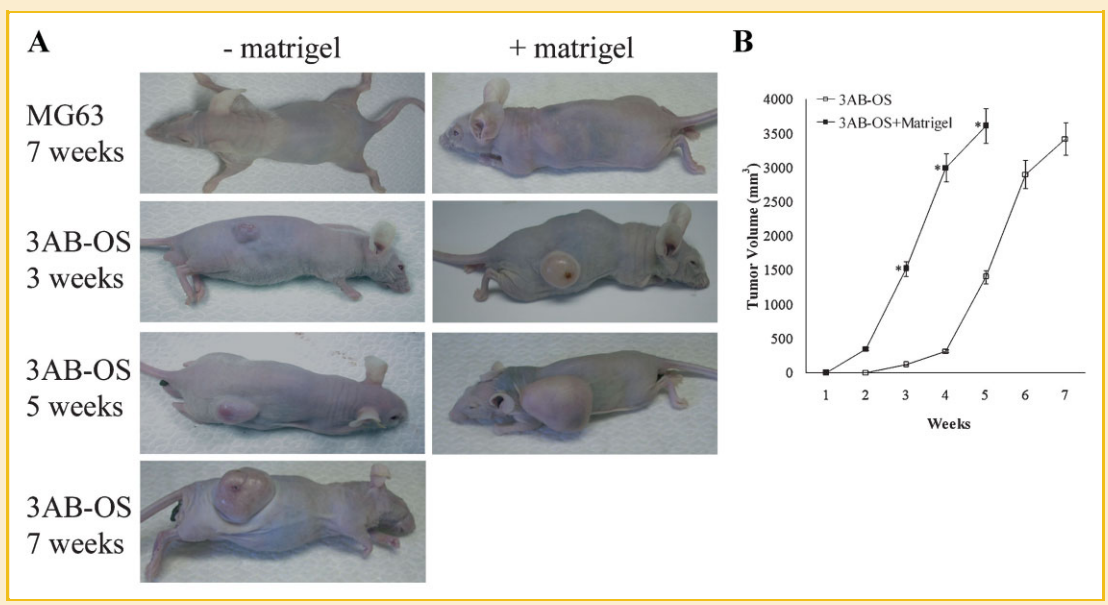

Fig. 1. Evaluation of in vivo tumorigenicity of MG63 cells and 3AB-OS CSCs. A: Xenograft formation in Fox1nu/nu mice. Representative images of mice sc-injected with either MG63 or 3AB-OS cells in the absence or presence of matrigel. B: Comparison of xenograft formation in vivo. Tumor volumes were measured and calculated each week. Tumor growth was plotted against time. Results are reported as mean ± SD. *P*-values were calculated with Student's *t*-test. Values of $^*P < 0.05$ were considered statistically significant.

However, tumor volume strongly depended on both the presence of matrigel and the engraftment time. More precisely, mice co-inoculated with 3AB-OS cells and matrigel, developed tumors, which were, at 3 and 5 weeks of engraftment, about 13 and 2.6-times greater than those found in mice inoculated with 3AB-OS cells alone. (Table I and Fig. 1A and B). As shown in Figure 1B, the trend of tumor growth over time in mice co-inoculated with 3AB-OS cells, with or without matrigel, was similar, although matrigel seemed to greatly accelerate both tumor engraftment and growth rate. Consistently, mice inoculated with 3AB-OS cells alone reached the endpoint (tumor weight had overcome 10% of the BW and mice were sacrificed for ethical reasons) at the 7th week after engraftment, whereas mice engrafted with the same cells in presence of matrigel were sacrificed at the 5th week.

Overall, Table I and Figure 1 show that, while MG63 cells do not possess tumor-forming ability in vivo, 3AB-OS cells are highly tumorigenic and matrigel greatly accelerated both tumor engraftment and growth rate. These results permitted to establish that the 3rd and 5th week of tumor engraftment in the presence of matrigel may be compared to the 5th and 7th week of tumor engraftment in the absence of matrigel. This statement was followed to describe the results reported in the successive paragraphs.

None of the engrafted mice ever developed clinical symptoms suggesting pathogenic human tumor cell dissemination in host tissues. To analyze whether tumor cells engraftment produced metastasis, internal organs of mice (heart, lungs, kidneys, spleen, liver, and brain) were removed, for macroscopic and microscopic analyses, following sacrifice. In our experiments, all inoculated mice remained healthy during the whole period of treatment and metastases were not observed in any of the studied animals. Figure 2 is a representative picture of mouse host tissues, analyzed both macroscopically (Fig. 2A) and microscopically after staining of FFPE sections with H&E (Fig. 2B), which shows the absence of any gross histological evidence of damage or cancer cell infiltration.

HISTOLOGY AND PROLIFERATIVE POTENTIAL OF TUMORS DERIVED FROM SUBCUTANEOUSLY INOCULATED 3AB-OS CSCS

First, to confirm that tumors derived from 3AB-OS cells engraftment were composed of human cells, tumor sections were stained with anti-human nuclear antigen monoclonal antibody. In addition, as a control for the specificity of the antibody against human antigens we used a section of mouse liver tissue. As shown in Figure 3A, the tumor section showed a strong reaction with the anti-human nuclear

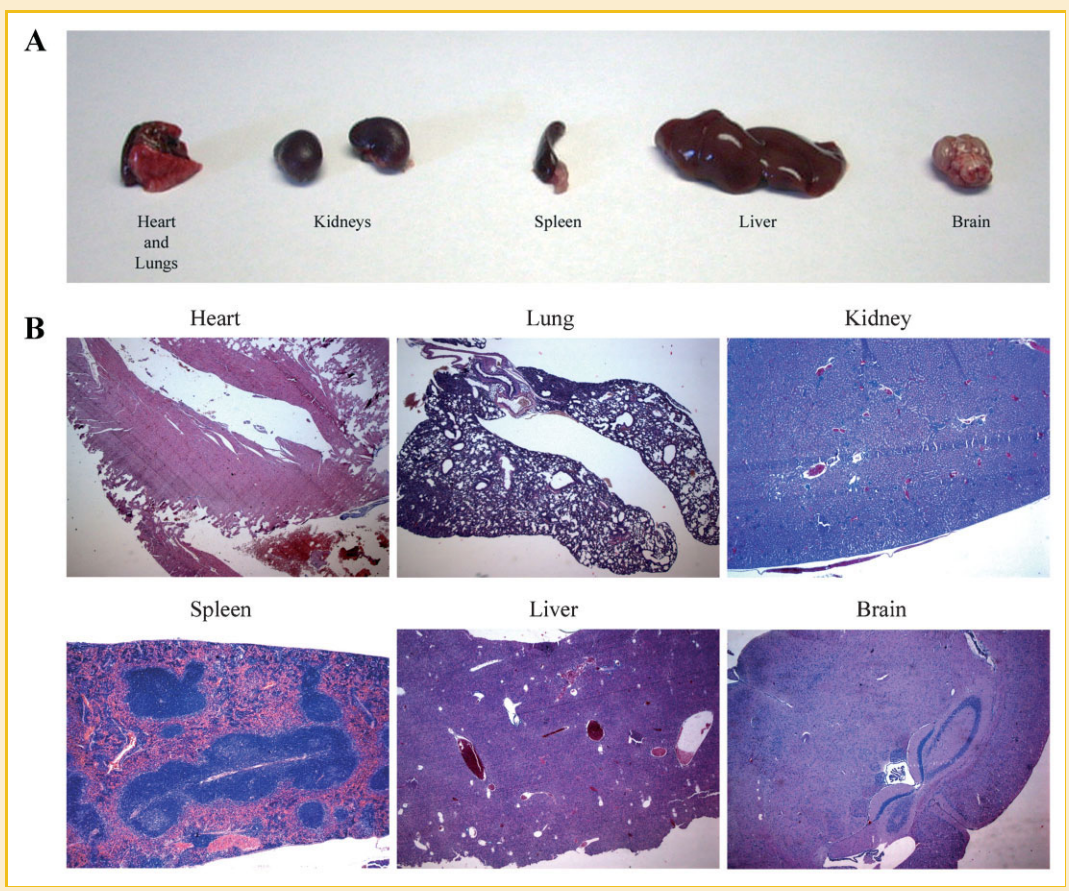

Fig. 2. Macroscopic and histological examination of internal organs of mice injected with either 3AB-OS or MG63 cells. A: Morphology of the internal organs (heart, lungs, kidneys, spleen, liver, and brain) removed from xenografted host mice. B: H&E staining of various host tissues (Original magnification, ×25).

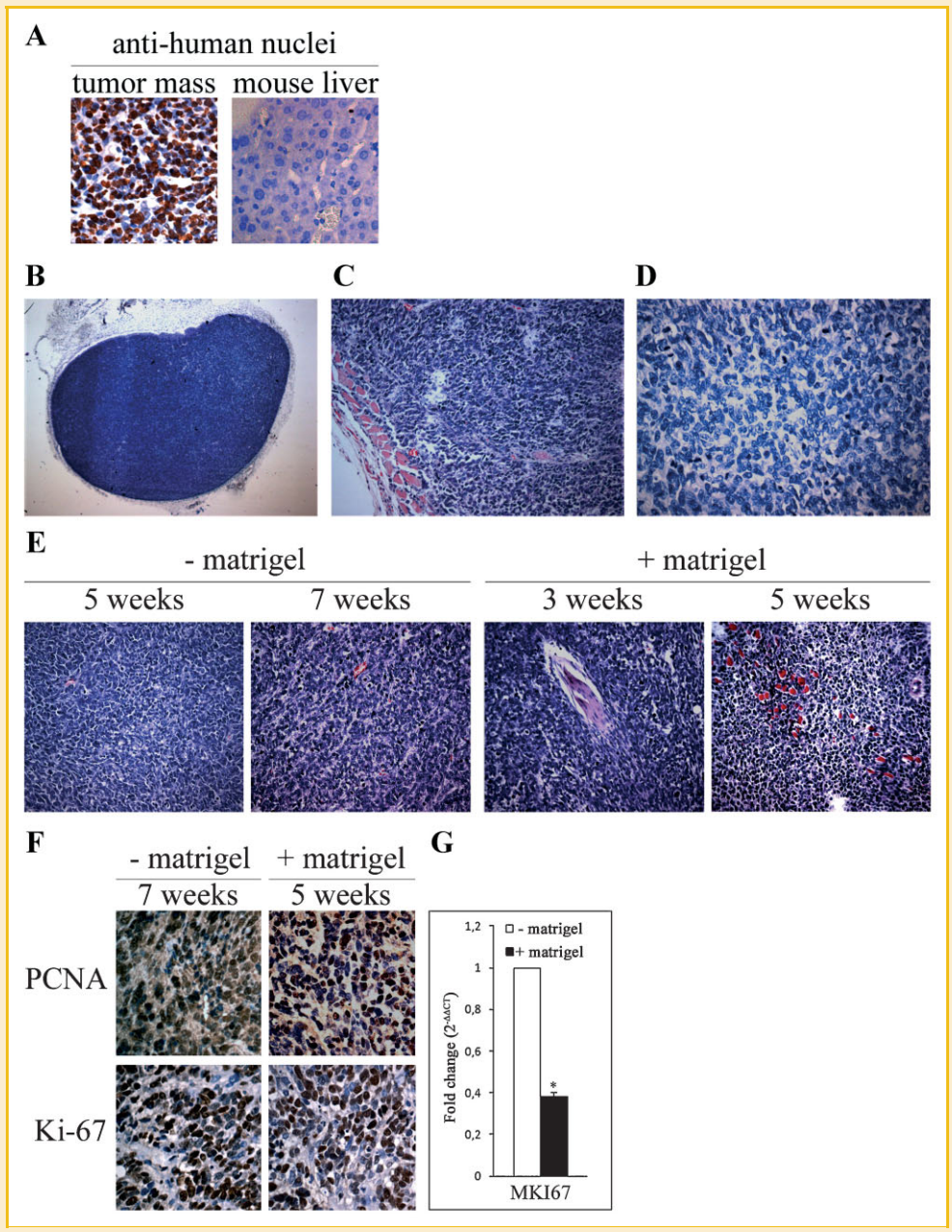

Fig. 3. Histology and proliferative potential of tumors derived from subcutaneously inoculated 3AB-OS CSCs. A: Staining of a tumor section with an anti-human antibody to establish the human origin of tumor cells. A liver mouse section was used as a negative control. B, C: Topography of a typical 3AB-OS-derived xenograft nodule after staining with H&E (Original magnification, ×25 and ×200, respectively). D: Mitotic figures of Toluidine-stained FFPE tumor sections (Original magnification, ×400). E: Histological analyses of tumors derived from mice injected with 3AB-OS cells either with or without matrigel at 3, 5, and 7 weeks of engraftment (H&E, Original magnification ×200). F: Tumor sections immunostained for PCNA (proliferating cell nuclear antigen) and Ki-67, two of the most frequently used cell proliferation markers. Comparison between the fifth week of 3AB-OS engraftment with matrigel and the 7th week 3AB-OS engraftment in its absence. G: Real-Time PCR analysis of MKI67. mRNA levels were normalized by β-actin. Data were expressed as mean ± SE. *P*-values were calculated using Student's *t*-test. Differences were considered significant at $^{*}P < 0.01$.

antigen antibody whereas no cross-reactivity was observed in the mouse liver section.

The analysis of 3AB-OS cell-derived tumor grafts has shown some common features that were evidenced in all experimental conditions (with or without matrigel; engraftment at 3, 5, or 7 weeks). Figure 3B–E, which includes representative pictures of the tumor microscopy, shows the gross microscopic appearance of the tumors that were circumscribed by a macroscopic fibrous capsule and pericapsular fibrosis, which was not involved in cell proliferation (Fig. 3B), and that became thinner during tumor growth (not shown). The tumors appeared well vascularized with several blood vessels passing through; cells contained large vesicular and empty-looking nuclei and a thick, distinct nuclear membrane, with coarse chromatin dispersion; the cytoplasm was

usually abundant and finely granular, basophilic, with no distinct cell border (Fig. 3C). Cells, which often appeared multinucleated, showed marked anaplasia—including abnormal forms—numerous mitotic figures (>6 to 40×), aberrant mitosis (Fig. 3D). However, tumors also showed some significant histologic differences which depended on the time of tumor development and the presence/absence of matrigel. Indeed (Fig. 3E), in the absence of matrigel, at 5 weeks after engraftment, tumors consisted of densely packed cells, sometimes with spindle-like shape, more frequently polygonal, mostly undifferentiated, without morphological organization, and with some blood vessels being visible. After 7 weeks, neoplastic cells showed crowding and overlapping, generated different patterns of organization, including bundles and vortexes, and a greater number of blood vessels crossed the tumor. When the tumors developed in the presence of matrigel, at 3 weeks after engraftment the cells appeared more densely packed than in the absence of matrigel, and polygonal and fusiform cells were much more numerous and organized into bundles that showed strong aspects of differentiation for the presence of muscle fibers. Cells in a rosette-like arrangement were also visible. After 5 weeks (which was the final endpoint for cells injected with matrigel, as reported in Fig. 1) aspects of differentiation were more numerous, a much greater number of blood vessels and multinucleated cells were present, and a larger number of muscle fibers crossed the tumor. Therefore, as matrigel seemed to provide a more favorable environment for tumor engrafment, cell growth and differentiation, we also assessed the proliferative state of the cells. To this purpose, tumor sections were immunostained for proliferating cell nuclear antigen (PCNA) and Ki-67, two of the most frequently used cell proliferation markers, which recognize nuclear antigens associated with all the phases of the cell-cycle except G0, with their maximal expression level during the S phase, nearby before the beginning of DNA synthesis [Muskhelishvili et al., 2003]. Comparing the 3rd week of tumor cell engraftment with matrigel with the 5th week of tumor cell engraftment in its absence, we observed a very high index of cell proliferation (with both PCNA and Ki-67 labelling indexes) with a few differences between the two conditions (Table II). Thereafter, cell proliferation index decreased and its level was much lower in tumor cells engrafted in the presence of matrigel (5th week) than in its absence (7th week, Fig. 3F and Table II).

Similar results were obtained also by comparing, through Real Time RT-PCR, mRNA extracted from FFPE tumors derived from engraftment in the presence and absence of matrigel. Indeed, the presence of matrigel decreased (−1.4-fold) the mRNA levels of MKI67, encoding the antigen identified by the Ki-67 monoclonal antibody (Fig. 3G).

Overall, these data suggest that matrigel, interacting with endogenous microenvironment might provide adequate cues to reduce cell proliferation.

CELL LINEAGE AND DIFFERENTIATION STATE OF TUMORS DERIVED FROM 3AB-OS CSCS ENGRAFTMENT

Cultured 3AB-OS cells possess pluripotent stem cell potential, as they are capable of giving rise—under specific inductive conditions—to cell derivatives of the three germ layers (ecto, endo, and mesoderm) [Vento et al., manuscript in preparation]. To evaluate whether 3AB-OS cells preserve in vivo these features of the cultured 3AB-OS cells, we assessed cell lineage and differentiation potential of engrafted 3AB-OS tumor cells (with and without matrigel), by immunohistochemical staining for GFAP (an ectodermal marker), vimentin (a mesodermal marker), and alfa-fetoprotein (an endodermal marker). As shown in both Figure 4 and Table III, at the 3rd week of 3AB-OS cell engraftment in the presence of matrigel, the percentage of tumor cell positivity for the three markers was markedly higher (71, 97, and 61% for GFAP, vimentin, and AFP, respectively) than in tumor cells at the 5th week of engraftment without matrigel (40, 13, and 30% for GFAP, vimentin, and AFP, respectively).

At the 5th week of engraftment in the presence of matrigel, the strong positive levels of the three markers were maintained, whereas in the corresponding samples (at the 7th week of engraftment without matrigel) positivity for the three markers markedly increased (64, 50, and 33%, respectively) thus that, at these engraftment times, a minor difference between the marker levels measured in the presence or absence of matrigel was observed.

Overall, these results suggest that engrafted 3AB-OS CSCs retain their differentiation potential. However, matrigel seems to induce a strong commitment to differentiation along the mesenchymal lineage, consistent with an increased morphological differentiation into muscle fibers, which is probably triggered by matrigel cooperation with the subcutaneous microenvironment.

EVALUATION OF MARKERS REQUIRED FOR STEM CELLS STATE

Our previous results [Di Fiore et al., 2009; Di Fiore et al., paper submitted] have shown that 3AB-OS cells express at high levels most crucial stemness markers (CD133, Oct3/4, hTERT, nucleostemin, Nanog, ABCG2, Lin28B, SOX2, Nestin, and HMGA2) known to be involved in the maintenance of the stem cell status. Here, we measured pluripotency and immortality markers by evaluating immunoreactivity of tumor cells, engrafted with and without

TABLE II. Evaluation of Cell Proliferation Index During Tumor Growth

	− Matrigel				+ Matrigel			
	5 weeks (positivity)		7 weeks (positivity)		3 weeks (positivity)		5 weeks (positivity)	
Cell Pro markers	% Mean ± S.D.	Degrees	% Mean ± S.D.	Degrees	% Mean ± S.D.	Degrees	% Mean ± S.D.	Degrees
PCNA	89.8 ± 4.3	+++	73.8 ± 2.7	++	98.8 ± 1.1	+++	42 ± 3.9	+
Ki-67	65.5 ± 3.1	++	53.2 ± 4.1	++	51 ± 2.2	++	31.1 ± 4.2	+

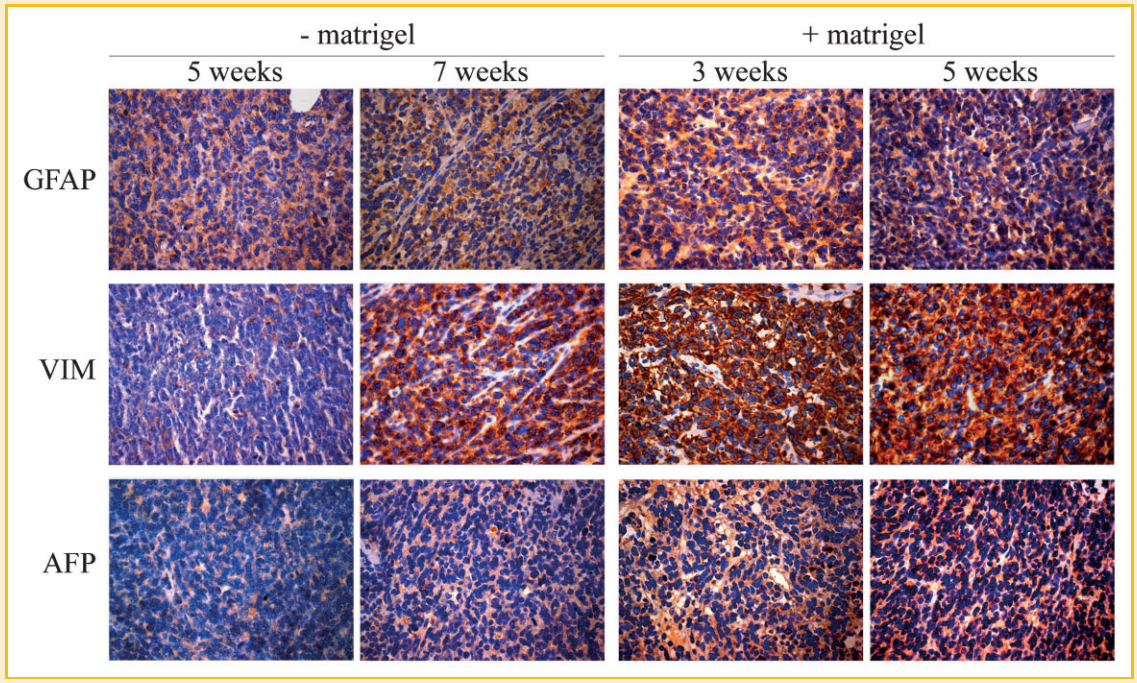

Fig. 4. Cell lineage and differentiation state of tumors derived from 3AB-OS CSC engraftment. Tumors at 3, 5, and 7 weeks of engraftment with or without matrigel. Immunohistochemical analyses of GFAP, vimentin, and α-fetoprotein expression. (Original magnification, ×400).

matrigel, versus the above reported genes. The results showed that, at the 3rd week of engraftment with matrigel no significant differences were found compared with the 5th week of engraftment without matrigel (not shown), whereas at the 5th week of engraftment with matrigel, tumors were much less immunoreactive than at the 7th week of engraftment without matrigel (Fig. 5A and Table IV). More precisely, as reported in the table, comparing the 5th week with matrigel to the 7th week without matrigel, the results show that in the presence of matrigel CD133 immunoreactivity decreased by 37.9%; Lin28B, ABCG2, SOX2, Nanog, and HMGA2, showed a decrease that ranged from 26 to 22%; Nucleostemin (NS), h-TERT, Nestin, and Oct3/4 showed a decrease that ranged from 20 to 17%. Comparing mRNA extracted from FFPE tumors, engrafted with and without matrigel, Real Time RT-PCR assays have shown (Fig. 5B) that in the presence of matrigel, mRNA levels of OCT4, Nanog, and CD133 were significantly lower than in its absence. Overall, these data suggest that matrigel might have provided the environmental cues for a gradual loss of stemness.

POTENTIAL SIGNALING PATHWAYS INVOLVED IN 3AB-OS CSCS TUMORIGENICITY

Unscheduled cell division is a characteristic of cancer cells. We have previously shown [Di Fiore et al., 2009] that 3AB-OS cells express higher levels of cell cycle checkpoint proteins (hyperphosphorylated/inactive pRb E2F1, cyclin D1, E, A, and B1, and cdc2) than parental MG63 cells. 3AB-OS cells also showed a much higher level of nuclear beta-catenin—known to control cyclin D1 expression—and express a greater number of proteins with anti-apoptotic activity (FlipL, Bcl-2, XIAP, IAP1, IAP2, and survivin).

Figure 6A and Table V—which describe immunohistochemical analyses of tumor cells at the 3rd week of engraftment in the presence of matrigel, show that tumor cells were strongly positive for the hyperphosphorylated/inactive pRb form (73%), cyclin D2 (85%), and c-Myc (74%). Similar results were obtained at the 5th week of engraftment without matrigel (Table V). These results indicated a potent activation of cell-cycle transitions, i.e., G1/S and G2/M, and suggested that signaling pathways involved in cell

TABLE III. Evaluation of Lineage-Related Markers During Tumor Growth

Lineage markers	− Matrigel				+ Matrigel			
	5 weeks (positivity)		7 weeks (positivity)		3 weeks (positivity)		5 weeks (positivity)	
	% Mean ± S.D.	Degrees	% Mean ± S.D.	Degrees	% Mean ± S.D.	Degrees	% Mean ± S.D.	Degrees
GFAP	40.2 ± 4.1	++	64.1 ± 3.1	++	70.7 ± 2.6	++	69.8 ± 3.9	++
VIM	12.8 ± 3.7	+	50.4 ± 1.4	++	96.6 ± 2.5	+++	95.4 ± 4.2	+++
AFP	30.6 ± 5.3	+	32.6 ± 1.7	++	60.6 ± 3.3	++	57.9 ± 4.5	++

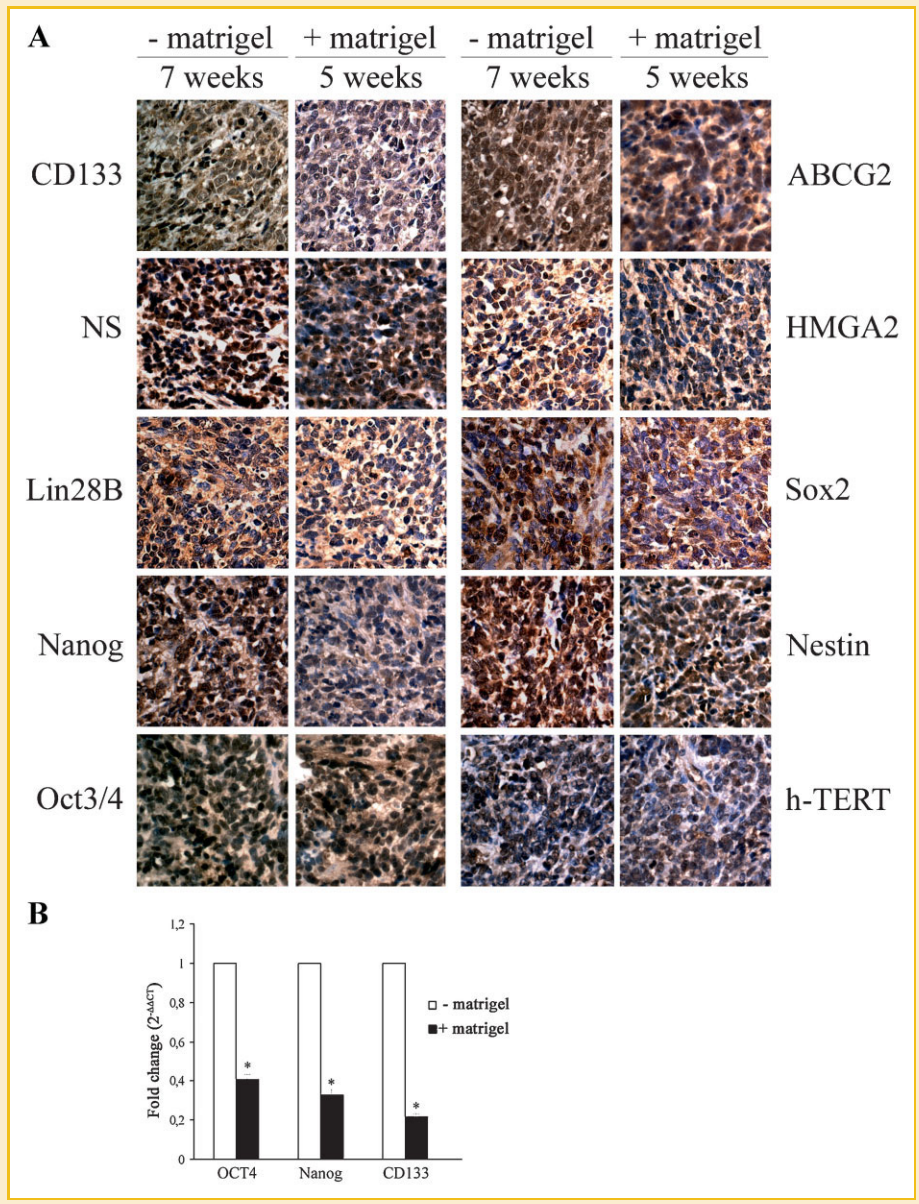

Fig. 5. Evaluation of markers required for Stem Cells State. A: Immunohostochemical analysis of CD133, nucleostemin (NS), Lin28B, Nanog, Oct3/4, ABCG2, HMGA2, SOX2, Nestin, and hTERT expression. (Original magnification, ×400). B: Oct4, Nanog, and CD133 mRNA levels were determined by real-time PCR analysis and normalized by β-actin. Data were expressed as mean ± SE. *P*-values were calculated using Student's *t*-test. Differences were considered significant at $^{*}P < 0.01$.

TABLE IV. Evaluation of Stem Cell-Related Markers During Tumor Growth

	− Matrigel		+ Matrigel	
	7 weeks		5 weeks	
Stem cells markers	% of positivity mean ± S.D.	Degrees of positivity	% of positivity mean ± S.D.	Degrees of positivity
CD133	98.3 ± 1.3	+++	61 ± 3.8	++
Lin28B	74.8 ± 3.6	+++	55.8 ± 4.7	++
ABCG2	98.4 ± 1.4	+++	72.1 ± 2.8	+++
SOX2	72 ± 0.8	+++	55 ± 2.6	++
Nanog	74.4 ± 4.3	+++	56.4 ± 3.3	++
HMGA2	80 ± 4.1	+++	62.5 ± 1.3	++
Nucleostemin (NS)	97.3 ± 2.5	+++	77.3 ± 5.5	+++
hTERT	64.9 ± 3.4	++	52.1 ± 0.4	++
Nestin	93.4 ± 2.8	+++	77.6 ± 4.8	+++
Oct3/4	91.3 ± 5.2	+++	75.2 ± 3.2	+++

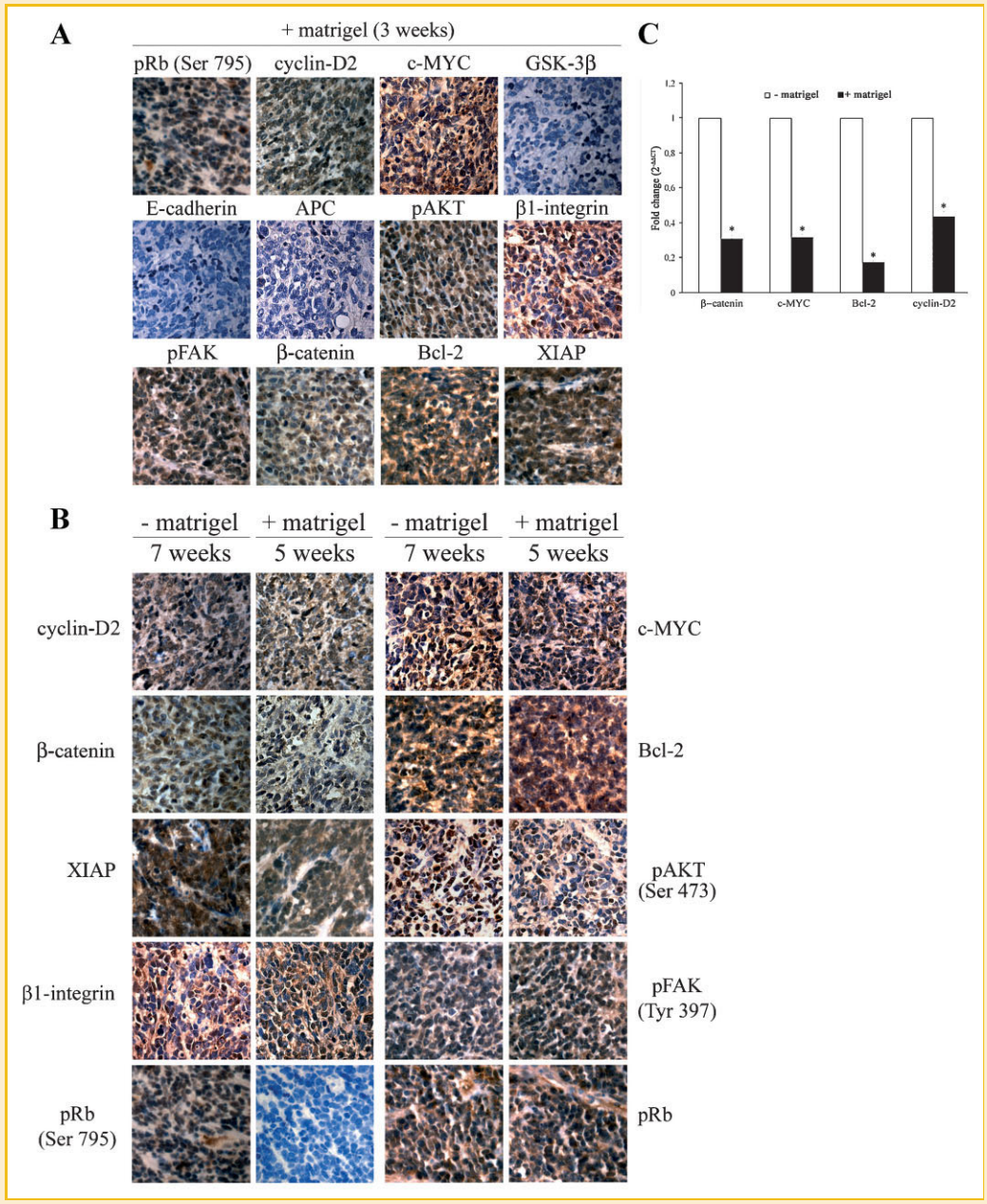

Fig. 6. Potential signaling pathways involved in 3AB-OS CSCs tumorigenicity. A: Tumors at 3 weeks of engraftment with matrigel. Immunohistochemical analyses of pRb (Ser 795), cyclin D2, c-Myc, GSK-3β, E-cadherin, APC, pAKT (Ser 473), β1-integrin, pFAK (Tyr 397), β-catenin, Bcl-2, and XIAP expression. (Original magnification, ×400). B: Tumors at 5, and 7 weeks of engraftment with or without matrigel. Immunohistochemical analyses of cyclin D2, c-Myc, β-catenin, Bcl-2, XIAP, pAKT (Ser 473), β1-integrin, pFAK (Tyr 397), pRb (Ser 795), and pRb expression. (Original magnification, ×400). C: Real-Time PCR analysis of β-catenin c-Myc, Bcl-2, and cyclin D2. mRNA levels were normalized by β-actin. Data were expressed as mean ± SE. *P*-values were calculated with Student's *t*-test. Differences were considered significant at $^{*}P < 0.01$.

survival, proliferation, and invasiveness might be preferentially activated in engrafted 3AB-OS cells. Analyses of Wnt and AKT signaling performed at the same weeks of engraftment described above showed that the cells were negative for GSK-3β, APC, and E-cadherin, suggesting that the canonical WNT signal is disrupted. Instead, cells were highly positive for β1-integrin (61%), pAKT (97%), pFAK (77%), and β-catenin (70%), with these three latter markedly accumulating in the nucleus. Moreover, cells were strongly positive for BCL-2 (96%) and XIAP (98%), thus evidencing the presence of potent antiapoptotic signals (Fig. 6A). Only a few differences were found comparing tumors engrafted at the 3rd and 5th week with and without matrigel (not shown). Conversely, by comparing the 5th week of engraftment with matrigel to the 7th week of engraftment without matrigel (Fig. 6B and Table V), immunohistochemical analyses showed that tumor cells were much less immunoreactive versus cyclin D2, c-Myc, and β-catenin in the

TABLE V. Potential Signaling Pathways Involving in the Tumorigenicity of 3AB-OS Cancer Stem Cells

Akt/Wnt pathway related markers	− Matrigel		+ Matrigel		− Matrigel		+ Matrigel	
	5 weeks (positivity)		3 weeks (positivity)		7 weeks (positivity)		5 weeks (positivity)	
	% Mean ± S.D.	Degrees	% Mean ± S.D.	Degrees	% Mean ± S.D.	Degrees	% Mean ± S.D.	Degrees
pRb (Ser 795)	70.2 ± 4.1	++	72.7 ± 2.6	+++	63.1 ± 2.6	++	–	
pRb	71.8 ± 3.7	+++	74.6 ± 2.5	+++	72.4 ± 2.5	+++	75.4 ± 4.2	+++
cyclin-D2	83.6 ± 5.3	+++	85.2 ± 3.8	+++	68.6 ± 3.8	++	57.9 ± 4.5	++
c-MYC	72.4 ± 3.3	+++	74.1 ± 3.6	+++	57 ± 3.6	++	39.4 ± 3.3	++
GSK-3β	–		–		–		–	
E-cadherin	–		–		–		–	
APC	–		–		–		–	
pAKT (Ser 473)	90.1 ± 2.6	+++	96.6 ± 1.7	+++	52.3 ± 1.7	++	35.2 ± 3.4	++
β1-integrin	59 ± 3.5	++	61 ± 4.3	++	55.4 ± 4.3	++	78.1 ± 3.3	+++
pFAK (Tyr 397)	74.3 ± 2.8	+++	77 ± 1.9	+++	65 ± 3.8	++	93 ± 4.4	+++
β-catenin	71,7 ± 3.8	+++	69,7 ± 5.8	++	61.7 ± 1.6	++	30.4 ± 2.3	++
Bcl-2	95.3 ± 3.4	+++	96.1 ± 2.5	+++	65.7 ± 3.7	++	44.1 ± 4.2	++
XIAP	97.5 ± 1.6	+++	98.2 ± 1.3	+++	75.7 ± 1.6	+++	45.8 ± 4.5	++

presence of matrigel than in its absence. Concomitantly, XIAP and Bcl-2 levels markedly decreased. In addition, in the presence of matrigel pAKT levels potently lowered, while β1-integrin and pFAK levels significantly increased with pFAK and pAKT significantly accumulating in the nucleus. Most intriguingly, in cells engrafted with matrigel hyperphosphorylated pRb levels became undetectable whereas the total pRb levels remained unchanged.

Comparing mRNA extracted from FFPE tumors produced by engraftment with and without matrigel, Real Time RT-PCR assay (Fig. 6C) showed that beta-catenin, c-Myc, Bcl-2, and Cyclin D2 expression potently decreased in the presence of matrigel.

Overall, these results suggest that pAkt, β1-integrin, and pFAK signaling pathways are crucial for 3AB-OS cells tumorigenicity. However, when tumor cells reach a high density, matrigel might provide the cues for both restraining cell proliferation and inducing myoblast differentiation.

DISCUSSION

To obtain preclinical results with high predictive value for clinical trials, it is crucial to have reliable in vivo tumor models on which new compounds and novel drug combinations can be evaluated [Céspedes et al., 2006; Troiani et al., 2008].

The CSC model represents nowadays an expanding field in cancer research that aims to identify the molecular mechanisms by which CSCs arise and acquire their stem-like characteristics and to establish how these cells can be selectively targeted and killed [Giordano et al., 2007].

Many established models of anti-tumor chemotherapy are based upon the successful propagation of established cell lines of human origin, as subcutaneous xenografts in athymic nude mice. However, although xenografts can provide valuable models for human cancers, many tumors can be difficult to establish [Sharkey and Fogh, 1984; Troiani et al., 2008] thus, the identification of factors that facilitate the growth of xenografts is of great interest. One possible way of improving such assay systems is the use of basement membrane components, as the extracellular matrices underlying epithelial cells (basement membranes) might influence cellular behavior through a variety of regulatory factors.

Matrigel is a solubilized tissue basement membrane matrix, extracted from the EHS mouse tumor, which resembles the complex extracellular environment found in many tissues. A number of articles have shown that matrigel can help to establish xenografts from a variety of cell lines [Topley et al., 1993].

In this study, aimed at obtaining a suitable in vivo model of human osteosarcoma CSCs, we have subcutaneously injected in athymic mice both 3AB-OS osteosarcoma CSCs (which we previously isolated from MG63 cells [Di Fiore et al., 2009], and the parental MG63 human osteosarcoma cells, either in the absence or in the presence of matrigel. We have shown that while MG63 cells do not possess tumor-forming ability in vivo, 3AB-OS cells instead were highly tumorigenic and matrigel greatly accelerated both tumor engraftment and growth rate.

Pluripotency and immortality in CSCs depend on the expression of a group of genes (stemness genes) which form a self-organized core of transcription factors required for maintaining stem cell-like features [Chen and Daley, 2008; Meng et al., 2012]. In particular, four factors (Oct4, Sox2, Nanog, and Lin28) are sufficient to reprogram human somatic cells to pluripotent stem cells showing the essential characteristics of embryonic stem (ES) cells [Yu et al., 2007]. These induced pluripotent human stem cells express telomerase activity, cell surface markers and genes that characterize human ES cells, and maintain the developmental potential to differentiate into advanced derivatives of all three primary germ layers [Cox and Rizzino, 2010].

We have previously shown that 3AB-OS cells have a strong stemness potential as they highly express a large panel of stemness-related genes, such as CD133, Nanog, Oct3/4, SOX2, h-TERT, HMGA2, Nucleostemin, ABCG2, Nestin, and Lin28B [Di Fiore et al., 2009; Di Fiore et al., paper submitted]. Here, we have shown that when 3AB-OS cells were engrafted in nude mice, they fully preserved their stemness features. Indeed, during the first weeks of engraftment, both in the presence and absence of matrigel, the stemness-related set of genes (including CD133, Nanog, SOX2, Oct3/4, h-TERT, HMGA2, Nucleostemin, ABCG2, Nestin, and Lin28B,) was

highly expressed. However, over time, matrigel presence in xenografts potently lowered the levels of these markers. Assessment of the tumor growth rate (tumor weight and volume measurements) and proliferation index (PCNA and Ki-67 analyses) showed that, during the first weeks of engraftment, both tumor growth and cell proliferation increased, thereafter, over time, these indices significantly lowered, with the presence of matrigel greatly accelerating these events. These findings suggested that matrigel, interacting with the microenvironment, might regulate tumor cell behavior providing the adequate cues for a gradual loss of stemness.

Genetic alterations and cytopathological heterogeneity characterize osteosarcomas and contribute to the intractability of the disease [Smida et al., 2010]. Osteosarcoma has been proposed to be a differentiation-flawed disease [Siclari and Qin, 2010]. In numerous tumors during cancer progression a partial or complete loss of E-cadherin has been described [Jeanes et al., 2008; Mohamet et al., 2011]. E-cadherin controls the levels of free-cytosolic β-catenin and loss of E-cadherin results in the disruption of cell–cell adhesion, in increased cytosolic and nuclear β-catenin levels and in increased cell proliferation. Loss of E-cadherin-mediated cell adhesion is one of the key mechanisms involved in metastasis and in epithelial-mesenchymal transition [Kalluri and Weinberg, 2009]. However, β-catenin level is also regulated by the β-catenin destruction complex (APC, Axin, GSK3b, and casein kinase), which modulates Wnt pathway through the GSK-3β-APC complex [MacDonald et al., 2009]. Alteration of this system leads to β-catenin stabilization and nuclear accumulation and the consequent transcription of genes (i.e., c-Myc and D cyclins) implicated in self-renewal [Ponce et al., 2011].

At present, we do not know how CSCs originate in osteosarcomas. However, the hypothesis that cancer arises from a tumorigenic subpopulation of CSCs that, during the course of tumorigenesis, accumulate multiple genetic alterations leading to an altered gene expression pattern [Gisselsson, 2011], generates the need to analyze CSCs for better understanding disease pathogenesis and for developing specific targeted therapy. We have previously shown [Di Fiore et al., 2009] that 3AB-OS cell cycle has an abbreviated G1-S phase accompanied by a strong G2-M transition. In particular, in 3AB-OS cells the pRb protein (which is known to influence the timing of G1-S) is constitutively inactivated through hyperphosphorylation and this is accompanied by high levels of nuclear β-catenin and a potent increase in cyclin D1 (responsible for mediating pRb phosphorylation) with an acceleration of the G1-S phase transition. In addition, 3AB-OS cells express high levels of cyclin B1 and cyclin-dependent kinases cdc-2, which promote G2-M phase transition. Moreover, 3AB-OS cells express many anti-apoptotic proteins (FlipL, Bcl-2, XIAP, IAP1, IAP2, and survivin). Overall, our findings suggest that 3AB-OS cells are endowed with a high proliferative capacity.

In this article, we have shown that engrafted tumor cells do not express E-cadherin, APC, and GSK-3beta, thus lacking the crucial regulators of soluble β-catenin levels. However, during the first weeks of engraftment they contain high levels of the phosphorylated form of AKT, pAKT, which has been reported to be necessary for the AKT-dependent up-regulation of β-catenin transcriptional activity [Tian et al., 2004; Fang et al., 2007; Ponce et al., 2011]. Consistently, engrafted tumor cells show high levels of nuclear β-catenin, c-Myc, and cyclin D2, along with the hyperphosphorylated-inactive pRb form, which confirms the lack of brakes to restrain cell proliferation. Similarly, the high levels of the antiapoptotic proteins, Bcl-2 and XIAP, show that the strong proliferative potential of the 3AB-OS cells was not counteracted by apoptosis.

Over time, significant changes were observed in the tumor cell composition of xenografts derived by 3AB-OS co-injection with matrigel. Tumors showed the appearance of blood vessels and muscle fibers that in large number crossed the cancer mass.

Understanding the molecular mechanisms controlling cell fate decisions in mammals is a major objective in CSC research. We have recently shown (paper in preparation) that 3AB-OS cells, under appropriate culture conditions, can be induced to differentiate into derivatives of all three primary germ layers. Here, measuring GFAP (ectodermal), vimentin (mesodermal), and AFP (endodermal) expression, we have shown that engrafted tumor cells fully preserved 3AB-OS multilineage commitment. In addition, a higher expression level of these markers was found in the presence of matrigel mixed cells or prolonging time of engrafment. However, the more interesting aspect concerns mesodermal commitment, as in the presence of matrigel engrafted 3AB-OS cells seemed to meet the appropriate environmental cues for committing along the mesenchymal lineage, with activation of myoblast differentiation. Differentiation of muscle progenitors is a multistep process that involves cell cycle withdrawal, expression of muscle-specific genes, and formation of multinucleated myofibers by cell fusion [Sun et al., 2004]. Moreover, it requires specific, but poorly understood, cell signals. Integrin β1 and FAK have been shown to be required for myoblast differentiation, especially for myotube formation and it has been shown that the integrin/FAK signaling pathway regulates the expression of the promyogenic factors, including MyoD [Han et al., 2011]. It is also known that myoblast differentiation requires dephosphorylation of the retinoblastoma pRb protein and that underphosphorylated pRb [Markiewicz et al., 2005] increases the transcriptional ability of MyoD family of muscle gene regulatory factors [Dick, 2007]. It has been proposed that a regulatory checkpoint in the terminal cell cycle arrest of myoblasts during differentiation involves the modulation of the cyclin D cdk-dependent phosphorylation of pRb through the opposing effects of cyclin D1 and MyoD [Kitzmann and Fernandez, 2001].

Here, we have shown that during the first weeks of engraftment tumor cells express high levels of β1-integrin along with phosphorylated FAK. Thereafter, in time—when in the presence of matrigel tumor cells appear to be enriched with blood vessels and muscle fibers—stemness, proliferative potential, and pAKT levels potently decreased, while β1-integrin and pFAK still increased with pFAK accumulating in the nuclei. Concomitantly, nuclear β-catenin, c-Myc, and cyclin D2 markedly decreased and hyperphosphorylated pRb forms became unmeasurable, whereas total pRb levels did not change, thus suggesting a potent increase in underphosphorylated pRb form. Our findings suggest that matrigel, interacting with the subcutaneous microenvironment, might regulate 3AB-OS cell behavior providing the adequate cues for transducing either oncogenic or differentiation signals transmitted by pAKT, integrin, and pFAK and supported by pRb protein.

For several malignancies, tumor xenografts in mice have proven to be reliable tools to predict drug response in vivo and the drug industry has recognized the potential utility of tumorgrafts for screening drug candidates. Our results provide for the first time a model of subcutaneous tumor engraftment with human osteosarcoma CSCs. Our novel model seems to have the appropriate characteristics to serve as a promising tool to investigate osteosarcoma stem cell features and for appropriately targeting CSCs by identifying links between the engrafted cells and their microenvironment.

ACKNOWLEDGMENTS

The authors wish to thank the Human Health Foundation (HHF), the Sbarro Health Research Organization (SHRO), and the Fondazione de Beaumont Bonelli for their support.

REFERENCES

Céspedes MV, Casanova I, Parreño M, Mangues R. 2006. Mouse models in oncogenesis and cancer therapy. Clin Transl Oncol 8:318–329.

Chen L, Daley GQ. 2008. Molecular basis of pluripotency. Hum Mol Genet 17(R1):R23–R27.

Clevers H. 2011. The cancer stem cell: Premises, promises and challenges. Nat Med 17:313–319.

Coffer PJ, Burgering BM. 2004. Forkhead-box transcription factors and their role in the immune system. Nat Rev Immunol 4:889–899.

Cox JL, Rizzino A. 2010. Induced pluripotent stem cells: What lies beyond the paradigm shift. Exp Biol Med 235:148–158.

Dick FA. 2007. Structure-function analysis of the retinoblastoma tumor suppressor protein - is the whole a sum of its parts? Cell Div 13(2):26.

Di Fiore R, Santulli A, Ferrante RD, Giuliano M, De Blasio A, Messina C, Pirozzi G, Tirino V, Tesoriere G, Vento R. 2009. Identification and expansion of human osteosarcoma-cancer-stem cells by long-term 3-aminobenzamide treatment. J Cell Physiol 219:301–313.

Euhus DM, Hudd C, LaRegina MC, Johnson FE. 1986. Tumor measurement in the nude mouse. J Surg Oncol 31:229–234.

Fang D, Hawke D, Zheng Y, Xia Y, Meisenhelder J, Nika H, Mills GB, Kobayashi R, Hunter T, Lu Z. 2007. Phosphorylation of beta-catenin by AKT promotes beta-catenin transcriptional activity. J Biol Chem 282:11221–11229.

Giordano A, Fucito A, Romano G, Marino IR. 2007. Carcinogenesis and environment: The cancer stem cell hypothesis and implications for the development of novel therapeutics and diagnostics. Front Biosci 12:3475–3482.

Gisselsson D. 2011. Intratumor diversity and clonal evolution in cancer–a skeptical standpoint. Adv Cancer Res 112:1–9.

Han JW, Lee HJ, Bae GU, Kang JS. 2011. Promyogenic function of Integrin/FAK signaling is mediated by Cdo, Cdc42 and MyoD. Cell Signal 23:1162–1169.

Jeanes A, Gottardi CJ, Yap AS. 2008. Cadherins and cancer: How does cadherin dysfunction promote tumor progression? Oncogene. 27:6920–6929.

Kalluri R, Weinberg RA. 2009. The basics of epithelial-mesenchymal transition. J Clin Invest 119:1420–1428.

Kitzmann M, Fernandez A. 2001. Crosstalk between cell cycle regulators and the myogenic factor MyoD in skeletal myoblasts. Cell Mol Life Sci 58: 571–579.

Li L, Neaves WB. 2006. Normal stem cells and cancer stem cells: The niche matters. Cancer Res 66:4553–4557.

MacDonald BT, Tamai K, He X. 2009. Wnt/beta-catenin signaling: Components, mechanisms, and diseases. Dev Cell 17:9–26.

Maitland NJ, Collins AT. 2008. Prostate cancer stem cells: A new target for therapy. J Clin Oncol 26:2862–2870.

Markiewicz E, Ledran M, Hutchison CJ. 2005. Remodelling of the nuclear lamina and nucleoskeleton is required for skeletal muscle differentiation in vitro. J Cell Sci 118:409–420.

Meng X, Neises A, Su RJ, Payne KJ, Ritter L, Gridley DS, Wang J, Sheng M, William Lau KH, Baylink DJ, Zhang XB. 2012. Efficient reprogramming of human cord blood CD34+ cells into induced pluripotent stem cells with OCT4 and SOX2 alone. Mol Ther 20:408–416.

Mohamet L, Hawkins K, Ward CM. 2011. Loss of function of E-cadherin in embryonic stem cells and the relevance to models of tumorigenesis. J Oncol 2011:352616.

Muskhelishvili L, Latendresse JR, Kodell RL, Henderson EB. 2003. Evaluation of cell proliferation in rat tissues with BrdU, PCNA, Ki-67(MIB-5) immunohistochemistry and in situ hybridization for histone mRNA. J Histochem Cytochem 51:1681–1688.

Nehls M, Kyewski B, Messerle M, Waldschütz R, Schüddekopf K, Smith AJ, Boehm T. 1996. Two genetically separable steps in the differentiation of thymic epithelium. Science 272:886–889.

Ponce DP, Maturana JL, Cabello P, Yefi R, Niechi I, Silva E, Armisen R, Galindo M, Antonelli M, Tapia JC. 2011. Phosphorylation of AKT/PKB by CK2 is necessary for the AKT-dependent up-regulation of beta-catenin transcriptional activity. J Cell Physiol 226:1953–1959.

Sharkey FE, Fogh J. 1984. Considerations in the use of nude mice for cancer research. Cancer Metastasis Rev 3:341–360.

Siclari VA, Qin L. 2010. Targeting the osteosarcoma cancer stem cell. J Orthop Surg Res 5:78.

Smida J, Baumhoer D, Rosemann M, Walch A, Bielack S, Poremba C, Remberger K, Korsching E, Scheurlen W, Dierkes C, Burdach S, Jundt G, Atkinson MJ, Nathrath M. 2010. Genomic alterations and allelic imbalances are strong prognostic predictors in osteosarcoma. Clin Cancer Res 16:4256–4267.

Sun L, Liu L, Yang XJ, Wu Z. 2004. Akt binds prohibitin 2 and relieves its repression of MyoD and muscle differentiation. J Cell Sci 117:3021–3029.

Ta HT, Dass CR, Choong PF, Dunstan DE. 2009. Osteosarcoma treatment: State of the art. Cancer Metastasis Rev 28:247–263.

Tian Q, Feetham MC, Tao WA, He XC, Li L, Aebersold R, Hood L. 2004. Proteomic analysis identifies that 14-3-3zeta interacts with beta-catenin and facilitates its activation by Akt. Proc Natl Acad Sci USA 101:15370–15375.

Tomayko MM, Reynolds CP. 1989. Determination of subcutaneous tumor size in athymic (nude) mice. Cancer Chemother. Pharmacol 24:148–154.

Topley P, Jenkins DC, Jessup EA, Stables JN. 1993. Effect of reconstituted basement membrane components on the growth of a panel of human tumour cell lines in nude mice. Br J Cancer 67:953–958.

Troiani T, Schettino C, Martinelli E, Morgillo F, Tortora G, Ciardiello F. 2008. The use of xenograft models for the selection of cancer treatments with the EGFR as an example. Crit Rev Oncol Hematol 65:200–211.

Ullman-Culleré MH, Foltz CJ. 1999. Body condition scoring: A rapid and accurate method for assessing health status in mice. Lab Anim Sci 49:319–323.

Wesolowski R, Budd GT. 2010. Use of chemotherapy for patients with bone and soft-tissue sarcomas. Cleve Clin J Med 77:S23–S26.

Yu J, Vodyanik MA, Smuga-Otto K, Antosiewicz-Bourget J, Frane JL, Tian S, Nie J, Jonsdottir GA, Ruotti V, Stewart R, Slukvin II, Thomson JA. 2007. Induced pluripotent stem cell lines derived from Human Somatic Cells. Science 318:1917–1920.